KERNFORSCHUNGSZENTRUM

KARLSRUHE

Oktober 1966

KFK 454
CN- 23/6

Institut für Angewandte Kernphysik

An Absolute (n,γ)-Cross-Section Measurement for Gold at 30 keV and Its Application in Normalization of Other Data

W. Pönitz

GESELLSCHAFT FÜR KERNFORSCHUNG M. B. H.

KARLSRUHE

KERNFORSCHUNGSZENTRUM KARLSRUHE

Oktober 1966

KFK 454
SN-23

Institut für Angewandte Kernphysik

An Absolute (n,γ)-Cross Section Measurement for Gold at 30 keV and Its Application in Normalization of Other Data

W. P. Pönitz

Gesellschaft für Kernforschung m.b.H. Karlsruhe

INTERNATIONAL ATOMIC ENERGY AGENCY

CONFERENCE ON NUCLEAR DATA -

MICROSCOPIC CROSS SECTIONS AND OTHER DATA BASIC FOR REACTORS

Paris, October 17 - 21, 1966

SN 23/6

AN ABSOLUTE (n,γ)-CROSS SECTION MEASUREMENT FOR GOLD AT 30 keV AND ITS APPLICATION IN NORMALIZATION OF OTHER DATA

W. P. Pönitz
Institut für Angewandte Kernphysik
Kernforschungszentrum Karlsruhe

1. Introduction

Due to the considerable importance of the neutron capture cross sections in the keV-energy region a large number of experiments were performed in the past by a variety of techniques. All available data of the (n,γ)-cross section of gold, which is of interest as a standard cross section, are shown in Fig. 1. As one can see, there is a considerable disagreement between the results of the different groups in both the absolute values and the shapes of the cross sections. In this paper we deal mainly with the (n,γ)-cross section of gold and describe a measurement at 30 keV neutron energy.

First of all we give in table I a review of the usable methods for capture cross section measurements in the keV-energy region. In Fig. 1 we have included the abbreviations given in table I. There are three main principles for the measurements of (n,γ)-cross sections in use: Firstly, the determination of

the transmission of neutrons through the sample which allows us to ascertain the loss of neutrons due to absorption if we take into consideration the scattered neutrons. Secondly, the measurement of the reaction rate in the sample due to the (n,γ)-process. Thirdly the observation of the decay of a neutron field in a "sample"-moderator. These main principles are sub-divided into a large number of methods differing in the kind of the determination of the transmission or the measurement of the reaction rate or the neutron flux.

An important feature of an (n,γ)-experiment is whether it is absolutely or relatively performed. The first class of experiments mentioned above and the last one are from their principle always absolute, whereas the second class is almost always only absolute if one determines the reaction rate and the neutron flux absolutely. However, we shall consider such methods as approximately absolutely performed which need only the well known (n,p)-scattering cross section (recoil proton measurements) or thermal absorption cross sections (integral methods).

The second method mentioned above we should sub-divide into a large number of methods which appear in the experiments. However, we have separated in table I the different methods for the determination of the reaction rate and those for the neutron flux. Generally all possible combinations of these methods are usable in an experiment.

2. A Measurement of $\sigma^{Au}_{n,\gamma}$ at 30 keV Neutron Energy

The experiment was carried out in two parts (s. Fig. 2):

1.) A gold foil (diameter 18 mm, thickness 0.3 mm) was irradiated using kinemetically collimated neutrons at the threshold of the $Li^7(p,n)\,Be^7$-reaction. The time dependence of the neutron flux was monitored by a long counter. At the end of the irradiation-time the γ-activities of the sample (Au^{198}; 411 keV-transition of Hg^{198*}) and

of the target (Be^7; 438 keV-transition of Li^{7*}) were measured using a 4 x 3 in NaI(Tl)-detector. To get the absolute disintegration rate in the Au-foil, a thin Au-foil was activated with thermal neutrons and its absolute disintegration rate measured by the $4\pi\beta$-γ-coincidence apparatus. This foil was used to calibrate the γ-detector. The different γ-self absorption in the thick and thin foil was calculated with the assumption of a homogenious activation in the foil.

2.) A LiF-target was placed at an end of a channel in the center of a glass sphere which was filled with $MnSO_4$-solution. The target was bombarded with a proton beam. The neutrons slow down and are captured partly at thermal energy by the Mn^{55}-nuclei. After the irradiation the solution was stirred and the γ-activity of a well-defined quantity was measured using a NaI(Tl)-detector. The arrangement used for this measurement was calibrated with a $MnSO_4$-solution of well-known activity which was previously determined by the $4\pi\beta$-γ-coincidence method. The Be^7-activity was measured in the same geometric arrangement as in the first experiment.

The relation between the various counts Z in the photo peaks of the transitions considered and the capture cross section of gold is given by the following relations:

$$Z_{Au} = \epsilon_{Au} \cdot Q_n \cdot d_{Au} \cdot F_{Au} \cdot \sigma_{n,\gamma} \qquad \text{First part of} \qquad (1a)$$

$$Z_{Be} = \epsilon_{Be} \cdot Q_n \cdot F_{Be} \qquad \text{the experiment} \qquad (1b)$$

$$Z_{Mn} = \epsilon_{Mn} \cdot C_{Mn} \cdot F_{Mn} \qquad \text{Second part of} \qquad (2a)$$

$$Z_{Be} = \epsilon_{Be} \cdot Q_n' \cdot F_{Be} \qquad \text{the experiment} \qquad (2b)$$

$$F = \frac{1}{\lambda}\left(1 - e^{-\lambda T}\right) \cdot \left(1 - e^{-\lambda \Theta}\right) \cdot e^{-\lambda t}.$$

ϵ being the probabilities to get counts in the photopeaks if decays take place. Q_n is the neutron source strength. N is the number of atoms per cm^3 and d the thickness of the gold foil. λ is the decay constant, T is the irradiation time, Θ is the counting time and t is the time between the end of the irradiation and the beginning of the counting. The activation of

the manganese nuclei, C_{Mn}, being determined by the neutron source strength Q_n' and given in a previous work /36/. ϵ_{Au} and ϵ_{Mn} are known from 4 ß-γ-coincidence measurements /25, 36, 47/. Thus we know from the second part of the of the experiment the factor ϵ_{Be} and use it to determine $\sigma^{Au}_{n,\gamma}$ from the first part.

However, there are a few effects which must be taken into account: The scattering of neutrons in the target backing plate, the activation of the foil due to neutrons which are scattered in the foil, the resonance self protection and the influence of the divergence of the neutrons in the cone. All these problems are discussed in a previous work /36/ and will not be repeated here. The result of the experiment is:

$$\sigma^{Au}_{n,\gamma} \text{ (30 keV)} = (0.598 \pm 0.012) \text{ barn.}$$

The advantage of the procedure used in this experiment in contrast to a previously described experiment /36/ is the use of a better geometric arrangement of the target and the manganese bath (this means a smaller loss of neutrons due to leakage at the edge of the manganese bath). Detailed values of the quantities defined in eqs. (1) and (2) are given in ref. 48.

3. "Best" Values for the Capture Cross Section of Gold at 30 keV

To get a normalization point for a capture cross section curve, we consider the independent measured values for gold around 30 keV given later than 1960. As "independent," we consider values which are not measured relative to other capture cross sections. The omission of relative measured values is well-motivated: We would like to avoid taking into account one measurement twice, at first directly and then again indirectly in a relative measurement. Not so very clear is the cut at 1960. Our argument was that the most measurements before are activation measurements and shell transmission measurements. For the shell transmission measurements, most authors have published newer results. The activation measurements depend on the absolute determination of the activities. The 4π ß-γ-coin-

cidence method, suggested by Campion [49] came into use around 1959 and gave rise to the determination of absolute activities on a new level.

Table II a contains a list of these independent cross section values at 30 keV. If no measured values are available at 30 keV we have used a smooth curve through the measured values and determined the error by the scattering and the errors of the values in the neighbourhood of 30 keV. We have omitted the values of Isakov et al. [39] because a renormalization was necessary and done by Konks et al. [27]. The original measured values of Moxon and Rae [21] we have averaged over an energy range of 5 keV.

Cross section values measured relative to the fission cross section of U 235 [18, 51] are included in our discussion; however, we have modified the original values by using the recent U 235 fission cross section values of White [52], determined relative to the n, p scattering cross section. The original results of experiments 1 to 14 (Table II a) are shown in Fig. 3.

First, we have calculated the non-weighted and the weighted average values of all data given in table II a. We note these values as "A", because it was not taken into consideration that several measurements depend upon the same method or calibration procedure.

In a second step, we have grouped the experiments according to the method for determination of the neutron flux, and have obtained a non-weighted average for each group (Table II b). The weighted average of the values No 15 - No 21 was noted as "B".

In a last step, we have selected some values: The research of D. Bogart and T.T. Semler [34] has shown recently that the Bethe-method for the calculation of the transmission for a spherical shell is not applicable if the cross sections (scattering and absorpiton) are not smooth. Therefore we omitt the value of

Belanova et al. [31] because in this work the assumption of smooth cross sections was made. Furthermore, we have omitted the value given by Cox [32]. This value makes use of the B^{10} (n,α)-cross section for high energies which is somewhat questionable. The values No 22 - 27 are calculated, in contrast to those of No 15 - 21, by weighting the single values. The value No 25 was evaluated using the value No 8 and the non-weighted average of No 11 and No 14, since these last two values are not independent. The value No 2 was corrected for activation by scattered neutrons (6.0 %).

To calculate the weighted average of the last group we have included an additional weight for the three cross section values based on absolute acitvation measurements. The average of this group was noted as "C" and used as a normalization value.
It is of interest that the several procedures to obtain an average value give almost identical results. We should remark that in the "C" average value the cross section No. 23 has the highest weight.

4. The Shape of the Capture Cross Section of Gold in the Energy Region 1 - 1000 keV

We have sub-divided the existing measurements of the (n,γ)-cross section shape of Au^{197} [1 - 36] in three groups: The first group contains all values measured below 30 keV and the third the values above 150 keV. The second group contains the experimental values between 30 and 150 keV. We have used smooth curves through the measured points and the values from these smooth curves at a number of energy points. All measured shapes within the first and the third groups are in fairly good agreement. Between 10 and 20 keV neutron energy the shape of the cross section measured by Gibbons et al. [15] and by Kompe [59] are in disagreement with the other measurements; this can be explained by the unfavourable true-to-background count ratios in these experiments in this region.

We have normalized these curves at 30 and 150 keV and calculated the average normalized values at all other energies in the two groups. The absolute value at 30 keV is given in the previous section.

The shape of the cross section in the second range and the absolute value at 150 keV are closely related. The shapes measured by Cox /32/, Miskel et al. /18/ and Harris et al. /30/ are in good agreement.between 30 and 150 keV, but if we normalize them at 30 keV, they give at 150 keV a value which is about 20 % lower than that of Barry /28/ and the values measured relative to $\sigma_{n,f}$ of U 235 /14, 18, 11, 5, 33/. The shape measured by Kompe /59/ relative to the cross section curve for the reaction $Li^6(n,\alpha)$ given by Schwarz et al. /60/ connects the absolute values at 30 and 150 keV mentioned above; however, the shape is in strong disagreement with all other measured values between 30 and 64 keV.

The situation seems to be unclarified up to now. We have used the following assumptions and procedure for deriving a "best" cross section curve: We assume that the values of Barry /28/ and those measured relative to the U 235 fission cross section are correct. For the cross section between 30 and 150 keV we have used a middle line between the curve given by Kompe /59/ (which depends on the data of Schwarz et al. /60/) and a curve which was constructed using the measured values up to 64 keV with a smooth connection between 64 keV and 150 keV. However, the curve is uncertain to $\pm$ 10 % in this range.

The calculated values of the capture cross section of Au^{197} and its errors are given in table III and shown in Fig. 4. In Fig. 4 we have included also fitted cross section curves given by Bogard /52/, Gibbons /53/ and Grench et al. /54/.

5. Renormalization of Capture Cross Sections of Several Elements

We have calculated the ratios $\sigma_{n,\gamma}^{X} / \sigma_{n,\gamma}^{Au}$ at several energy points using smooth curves through the measured values of $\sigma_{n,\gamma}^{X}$ and $\sigma_{n,\gamma}^{Au}$ given in ref. 1 - 38, 55, 56, 57, 58. All available ratios are averaged and multiplied by the values of $\sigma_{n,\gamma}^{Au}$ determined in the previous section. The results for smooth curves of the capture cross sections of Mo, Rh, Ag, In, Sb, I, Ta and W are given in table III. The errors are estimated by the scattering of the different cross section ratios and by the errors of the gold cross section. The results are shown in Fig. 5.

6. Discussion

The problem of finding an absolute cross section value in the keV-neutron energy region usable for the normalization of cross section curves, seems to be - at least in the author's opinion - solved. However, there are disagreements in the shape of the (n,γ)-cross section of gold between 30 keV and 150 keV which can not be explained up to now. Therefore it is not possible to give a standard cross section in the energy range 1 - 1000 keV which is better than 7 - 12 %.

The accuracies of the (n,γ)-cross sections of several other materials considered in this paper are not strongly affected by the uncertainty of the standard cross section , because the ratios $\sigma_{n,\gamma}^{X} / \sigma_{n,\gamma}^{Au}$ measured by different authors disagree generally about 10 - 30 %.

In conclusion the author thanks H.W. Schmitt for valuable discussions and Prof. K.H. Beckurts for his interest in these investigations.

[1] HENKEL, R.L., BARSCHALL, H.H., Phys. Rev. 80 (1950) 145.

[2] HUMMEL, V., HAMERMESH, B., Phys. Rev. 82 (1951) 67.

[3] MACKLIN, R.L., LAZAR, N.H., LYON, W.S., Phys. Rev. 107 (1957) 504.

[4] BOOTH, R., BALL, W.P., McGREGOR, M.H., Phys. Rev. 112 (1958) 226

[5] JOHNSRUD, A.E., SILBERT, M.G., BARSCHALL, H.H., Phys. Rev. 116 (1959) 927.

[6] FERGUSON, A.T.G., PAUL, E.B., J. Nucl. Energy A10 (1959) 19.

[7] LYON, W.S., MACKLIN, R.L., Phys. Rev. 114 (1959) 1619.

[8] BAME, S.J., CUBITT, R.L., Phys. Rev. 113 (1959) 256.

[9] BILPUCH, E.G., WESTON, L.W., NEWSON, H.W., Ann. of Physics 10 (1960) 455

[10] BLOCK, R.C., SLAUGHTER, G.G., WESTON, L.W., VONDERLAGE, F.C., Neutron Time-of-Flight Methods (J. SPAEPEN, Ed.) EURATOM, Brussels (1961) 203.

[11] DIVEN, B.C., TERRELL, J., HEMMENDINGER, A., Phys. Rev. 120 (1960) 556.

[12] SCHMITT, H.W., COOK, C.W., Nucl. Physics 20 (1960) 202.

[13] WESTON, L.W., LYON, W.S., Phys. Rev. 123 (1961) 948.

[14] COX, S.A., Phys. Rev. 122 (1961) 1280.

[15, 16, 17] GIBBONS, J.H., MACKLIN, R.L., MILLER, P.D., NETLER, J.H., Phys. Rev. 122 (1961) 182.

[18] MISKEL, J.A., MARSH, K.V., LINDNER, M., NAGLE, R.J., Phys. Rev. 128 (1962) 2717.

[19] BERGQUIST, I., Ark. Fys. 23 (1963) 425.

[20] HADDAD, E., WALTON, R.B., FRIESENHAHN, S.J., LOPEZ, W.M., Nucl. Instr. 31 (1964) 125; EANDC-33 "U" (1963).

[21] MOXON, M.C., RAE, E.R., Nucl. Instr. 24 (1963) 445.

[22] MACKLIN, R.L., GIBBONS, J.H., INADA, T., Nucl. Phys. 43 (1963) 353.

/23/ SCHMITT, H.W., EANDC-33 "U" (1963) 41.

/24/ POENITZ, W.P., EANDC-33 "U" (1963) 164.

/25/ POENITZ, W.P., BRUDERMUELLER, G., EANDC-33 "U" (1963) 87.

/26/ LANGSDORF, A., LANE, R.O., ELWYN, A.J., WASH-1046 (1964).

/27/ KONKS, V.A., POPOV, Y.P., SHAPIRO, F.L., Soviet Phys. (JETP) 19 (1964) 59.

/28/ BARRY, J.F., J. Nucl. Energy. A/B 18 (1964) 491.

/29/ CHAUBEY, A.K., SEHGAL, M.S., Nucl. Phys. 66 (1965) 267.

/30/ HARRIS, K.K., GRENCH, H.A., JOHNSON, R.G., VAUGAN, F.J., FERZIGER, J.H., SHER, R., Nucl. Phys. 69 (1965) 37

/31/ BELANOVA, T.S., VANKOV, A.A., MIKHATLUS, F.F., STAVISSKII, Y.Y., J. Nucl. Energy A/B 20 (1966) 411; Atomnaya Energiya 19 (1965) 3.

/32/ COX, S.A., WASH-1068 (1966) 6.

/33/ GRENCH, H.A., COOP, K.L., MENLOVE, H.O., VAUGHN, F.J., WASH-1068 (1966) 75.

/34/ BOGART, D., SEMLER, T.T., NASA TM X-52173

/35/ RYVES, T.B., ROBERTSON, J.C., AXTON, E.J., GOODLER, I., WILLIAMS, A., J. Nucl. Energy A/B 20 (1966) 249.

/36/ POENITZ, W.P., EANDC(E)-69 "S"; J. Nucl. Energy, to be published (1966).

/37/ KONONOV, V.N., STAVISSKII, I.I., TOLSTIKOV, V.A. Soviet J. Atom. Energ. 5 (1958) 1483.

/38/ BELANOVA, T.S., Soviet J. Atom. Energ. 8 (1960) 462.

/39/ ISAKOV, A.I., POBOV, Y.P., SHAPIRO, F.L., Sov. Phys. (JETP) 11 (1960) 712.

/40/ BETL, H., LE RIGOLEUR, M., LEROY, J.L., EANDC-33 "U" (1963), 150.

/41/ POENITZ, W.P., WATTECAMPS, E., EANDC-33 "U" (1963), 102.

/42/ GONDE, H., SCHWARZ, S., SFARFELT, N., Ark. f. Fysik 39 (1965) 45

/43/ BECKURTS, K.H., IAK 3/63, Kernforschungszentrum Karlsruhe (1963).

/44/ MITZEL, F., PLENDL, H.S., Nukleonik 6 (1964) 371.

/45/ BECKURTS, K.H., IAK 13/64, Kernforschungszentrum Karlsruhe (1964).

/46/ MIESSNER, H., ARAI, E., Nukleonik, to be published.

/47/ POENITZ, W.P., KFK-180 (1963).

/48/ POENITZ, W.P., Thesis, Karlsruhe (1966).

/49/ CHAMPION, P.J., Measurements and Standards of Radioactivity National Science Series Report 24, Publication No 573

/50/ WHITE, P.H., J. Nucl. Energy A/B 19 (1965) 325

/51/ KNOLL, G.F., POENITZ, W.P., to be published.

/52/ BOGART, D., NASA TM X-52 162 (1966).

/53/ GIBBONS, J.H., see ref. 54.

/54/ GRENCH, H.A., COOP, K.L., MENLOVE, H.O., VAUGHN, F.J. to be published.

/55/ COX, S.A., Phys. Rev. 133 (1964) B378.

/56/ HUGHES, D.J., SCHWARTZ, R.B., BNL-325 (1958).

/57/ GORDEEV, I.W., KARDASCHEV, D.A., MALUESCHEV, A.W., INDSWG-43 (1963)

/58/ POPOV, U.P., Tpygir ØUAN TaM XXIV (1964)

/59/ KOMPE, D., this conference, contribution CN-23/10.

/60/ SCHWARZ, S., STROEMBERG, L.G., BERGSTROEM, A., Nucl. Phys. 63 (1965) 593.

Figure Captions

Fig. 1. The neutron capture cross section of gold. Comparison of existing data.

Fig. 2. Experimental set-up.

Fig. 3. The independent experimental values of $\sigma^{Au}_{n,\gamma}$ at 30 keV neutron energy.

Fig. 4. Comparison of fitted cross section curves.

Fig. 5. Capture cross sections of Mo, Rh, Ag, In, Sb, I, Ta and W in the energy range 1 - 1000 keV

TABLE I Experimental Methods for Capture Cross Section Measurements

Principle	Abbreviation	Method	Remarks	Ref.
Transmission (Absorption)	SST	Spherical Shell Transmission	The transmission of a spherical shell is observed. In contrast to a normal transmission experiment, in this geometric arrangement the neutrons which are "scattered out" by that part of the sample which is between the source and the detector are compensated by neutrons which are"scattered in" from the rest of the sample.	12, 23, 31, 38, 34 and refe-rences cited therein
	CCD	Cross Section Difference Method	The normal transmission due to absorption and scattering in a sample is observed. In addition the scattered neutrons are measured in a 4π geometry. To eleminate the efficiency of the 4π -detector the same experiment is performed with a "pure" scatterer.	26
	TA	Total Absorption Method	The loss of neutrons due to a sample in a 4π -neutron detector is measured. This method is in principle identical with the method to determine the resonance integral given by Popov.	31
Reaction (Capture)	F	Neutron	Flux Measurements	
	F-RP	Recoil Proton	The well-known (n,p)-scattering cross section is used to determine the neutron flux. Because it is difficult to measure the recoil protons for low energies, the lowest neutron energy for which absolute neutron flux measurements have been performed is about 40 keV	28
	F-AA	Associate Activity	The associated activity (nucleus B) in the neutron source reaction A(B,n)B being measured and is equal to the neutron source strength. If the (n,γ)-reaction at the sample leads to an activity which is similar to those of the source reaction, the combination F-AA/C-A is an absolute method.	24, 30, 36

TABLE I (Continued)

Principle	Abbreviation	Method	Remarks	Ref.
Reaction (Capture)	F-AP	Associate Partical	The associated (charged) particle in the source being dedetected. This method was not performed for measurements in the keV-energy region, as far as we know, up to now.	40
	F-ID	Integral Detectors	The neutrons are slowed down in a large moderator and detected at thermal neutron energy in the whole moderator. This means a flat response of the detector as a function of the incident neutron energy. The detector being calibrated in energy regions where good methods for flux measurements exist. (Examples: Long Counter, Macklin sphere, grey neutron detector, large liquid scintillator with a scatterer)	3, 6, 9, 13, 41, 42
	F-IM	Integral Methods (mainly $MnSO_4$-bath technique)	The principle of neutron slowing down is the same as for F-ID. However, the captures at thermal energies lead partly to an activity which can be measured absolutely. This activity together with the ratio of the activation cross section to the capture cross section of the moderator determine the neutron flux.	25, 35, 36
	F-R or F-U235	Relative Measurements	The neutron flux measurement is avoided by using an (n,γ)-cross section or the (n,f)-cross section of U235 as a standard	4, 5, 8, 9, 10, 11, 15, 18, 22, 29, 32, 33

TABLE I (Continued)

Principle	Abbreviation	Method	Remarks	Ref.
	F-B10	Relation to $B^{10}(n,\alpha)$	This procedure is different from F-R in as much as the thermal cross section and an assumption about the energy dependence of the cross section (1/v-behaviour) is used. Furthermore the measurement of the (n,α)-cross section for B^{10} using the spherical shell transmission method, in contrast to the (n,γ)-measurements, allows the assumption of smooth cross sections in the keV-energy region.	9, 10, 14, 20, 21, 27, 32, 39, 44
	F-SD	Slowing down spectrometer	In principle it should be possible to calculate the neutron flux in a large moderator of heavy nuclei as a function of time (energy) using a pulsed neutron source of constant source energy. A calibration at one energy would determine the flux at all energies. However, this method has not been used in absolute cross section determination; rather all measurements have been made relative to B10.	43
Reaction (Capture)	C	Capture rate measurements		
	C-LLS	Total absorption of prompt γ-rays large liquid scintillator)	The prompt γ-rays are detected in a 4π-geometry using a large liquid scintillator tank. To obtain independence of the efficiency from the changes of the γ-multiplicities in the cascades, it is necessary to use a large scintillator volume.	11, 15, 10, 20

TABLE I (Continued)

Principle	Abbreviation	Method	Remarks	Ref.
Reaction (Capture)	C-EPD	Detection of prompt γ-rays proportional to their energy	The efficiency for the detection of a prompt γ-ray in the cascade is proportional to the energy of this γ-ray. This means that the overall efficiency is independent of the multiplicity in a γ-ray cascade and only proportional to the max. γ-transition energy. (Examples: Proportional Counter; Moxon-Rae detector)	21, 27 39, 44
	C-LVD	Detection of prompt γ-rays in large volume Scintillation Counters	The prompt γ-rays are detected in only a part of the 4π -angle with a large volume scintillation detector. However, most of the detectors are not "black" for the γ-rays and therefore are sensitive to a change in the γ-ray spectra. (Examples: Plastic Scintillators, CaF-Crystals, NaI-crystals)	19
	C-A	Activation	The activity of a sample due to (nγ)-reactions is determined after the irradiation. Not all stable nuclei yield a radioactive nucleus when undergoing an n,γ reaction; also in many cases it is not possible (because of half-life and/or decay scheme) to determine the induced activity. Therefore the application of this method to the determination of (n,γ) cross sections is very restricted. However, in a few cases such precise determination of the activity (that is, also of the capture rate) are possible, that this method is very favourable for absolute cross section measurements.	1 - 9 13, 14, 18, 24, 25, 28 33, 35, 36

TABLE I (Continued)

Principle	Abbreviation	Method	Remarks	Ref.
Reaction (Capture)		Relation to capture rates at thermal or eV energy	The elimination of the detector efficiency (in the cases C-LLS, C EPD, C-LVD and C-A) is possible if one knows either the capture cross section at thermal neutron energy or the resonance parameters.	4, 20 21, 27, 39, 44
Decay Time Measurement (Absorption)	DTM	Neutron field decay time measurement.	The decay time constant $\alpha_o = v_o \Sigma_a + D_o B^2 + CB^4$ is observed to determine the absorption cross section Σ_a. The moderation effect must be taken into consideration. The result is an effective cross section averaged over many resonances.	45, 46

TABLE II a) Experimental Cross Section Values at 30 keV

No	Authors	Ref.	Year	Methods, Remarks	Value/barn
1	Weston Lyon	13	1961	F-ID/C-A	0.767 ± 0.060
2	Miskel et al.	18	1962	F-U235/C-A	0.880 ± 0.090
3	Moxon, Rae	21	1963	F-B10/C-EPD Calibration at several resonances	0.600 ± 0.060
4	Haddad et al.	20	1964	F-B10/C-LLS Calibration using the 1.46 eV-resonance of Au	0.525 ± 0.100
5	Konks et al.	27	1964	F-B10/C-EPD Calibration using thermal cross section and resonance parameter of Au	0.630 ± 0.120
6	Harris et al.	30	1965	F-AA+C-A	0.640 ± 0.040
7	Pönitz	48, 36	1966 (Jan.)	F-AA+C-A	0.593 ± 0.012
8	Pönitz	48, 36	1966 (Jan.)	F-IM/C-A	0.604 ± 0.011
9	Schmitt Cook, Bogart, Semler	12, 34	1966 (March)	SST (Monte Carlo calculation)	0.608 ± 0.050 (b)
10	Cox	14, 32	1966 (March)	F-B10, F-U235/C-A	0.809 ± 0.080
11	Ryves et al.	35	1966 (April)	F-IM/C-A	0.555 ± 0.040 (b)
12	Belanova et al.	31	1966 (May)	TA, SST (Bethe method)	0.500 ± 0.050 (b)
13	Knoll, Pönitz	51	1966 (Aug.)	F-U235/C-A The cross section ratio given in the referred work and an extrapolated value of $\sigma_{n,\gamma}$ given by White /30/ was used	0.608 ± 0.040
14	This work	-	1966	F-IM/C-A	0.598 ± 0.012

(a) The original values are averaged at an energy range of 5 keV

(b) The values are translated from 24.8 keV to 30 keV using the cross section curve given by Harris et al. /30/.

TABLE II b) Reduced and Selected Cross Section Values at 30 keV and Average Values

No	No from Tab. II a	Method	Value/barn
15	1	F-ID/C-A	0.767 ± 0.060
16	3, 4, 5	F-B10/C-EPD, C-LLS	0.585 ± 0.095
17	6, 7	F-AA+C-A	0.617 ± 0.026
18	8, 11, 14	F-IM/C-A	0.586 ± 0.021
19	9, 12	SST	0.554 ± 0.050
20	2, 13	F-U235/C-A	0.749 ± 0.065
21	10	F-B10, F-U235/C-A	0.809 ± 0.080

No	No from Tab. II a	Method	Add. Weight	Value/barn
22	1	F-ID/C-A	0.3	0.767 ± 0.060
23	3, 4, 5	F-B10/C-EPD, C-LLS		0.587 ± 0.021
24	6, 7	F-AA+C-A		0.598 ± 0.030
25	8, 11, 14	F-IM/C-A	0.3	0.595 ± 0.030
26	9	SST		0.608 ± 0.050
27	2, 13	F-U235/C-A	0.3	0.644 ± 0.021

No	No from above	Notation	Average value /barn
I	1 - 14	"A" non-weighted	0.623 ± 0.030
Ia	1 - 14	"A" weighted	0.600 ± 0.009
II	15 - 21	"B" weighted	0.615 ± 0.025
III	22 - 27	"C" weighted	0.603 ± 0.012

TABLE III - Capture Cross Section Values in the Energy Region 1 - 1000 keV

	σ/barn								
E/keV	Au	Mo	Rh	Ag	In	Sb	I	Ta	W
1	6.77	0.72	2.82	4.27	2.59	2.13	3.38	10.16	2.49
2	4.08	0.63	2.35	2.91	2.18	1.43	2.50	6.33	1.43
3	3.03	0.56	2.09	2.44	1.98	1.16	2.15	4.61	1.06
5	2.11	0.47	1.73	1.94	1.65	0.91	1.68	3.16	0.75
10	1.31	0.33	1.27	1.52	1.29	0.69	1.17	1.83	0.49
20	0.811	0.234	1.00	1.28	1.02	0.574	0.90	1.18	0.364
30	0.603	0.165	0.85	1.02	0.81	0.480	0.72	0.85	0.292
50	0.460	0.110	0.72	0.85	0.65	0.370	0.570	0.65	0.250
70	0.400	0.090	0.64	0.73	0.56	0.285	0.460	0.545	0.220
100	0.355	0.076	0.54	0.61	0.46	0.216	0.375	0.460	0.192
200	0.304	0.062	0.364	0.406	0.321	0.145	0.246	0.321	0.132
300	0.245	0.056	0.258	0.310	0.287	0.130	0.197	0.256	0.113
500	0.159	0.045	0.150	0.198	0.267	0.114	0.142	0.182	0.095
700	0.118	0.036	0.103	0.150	0.267	0.106	0.102	0.145	0.090
1000	0.093	0.027	0.075	0.112	0.269	0.111	0.073	0.119	0.098
	$\Delta\sigma/\sigma$ / %								
1-10	7	30	20	10	15	30	20	10	15
10-40	8	20	20	10	10	20	15	10	15
40-200	12	20	20	15	15	15	15	15	15
200-1000	7	20	15	10	15	20	20	20	15

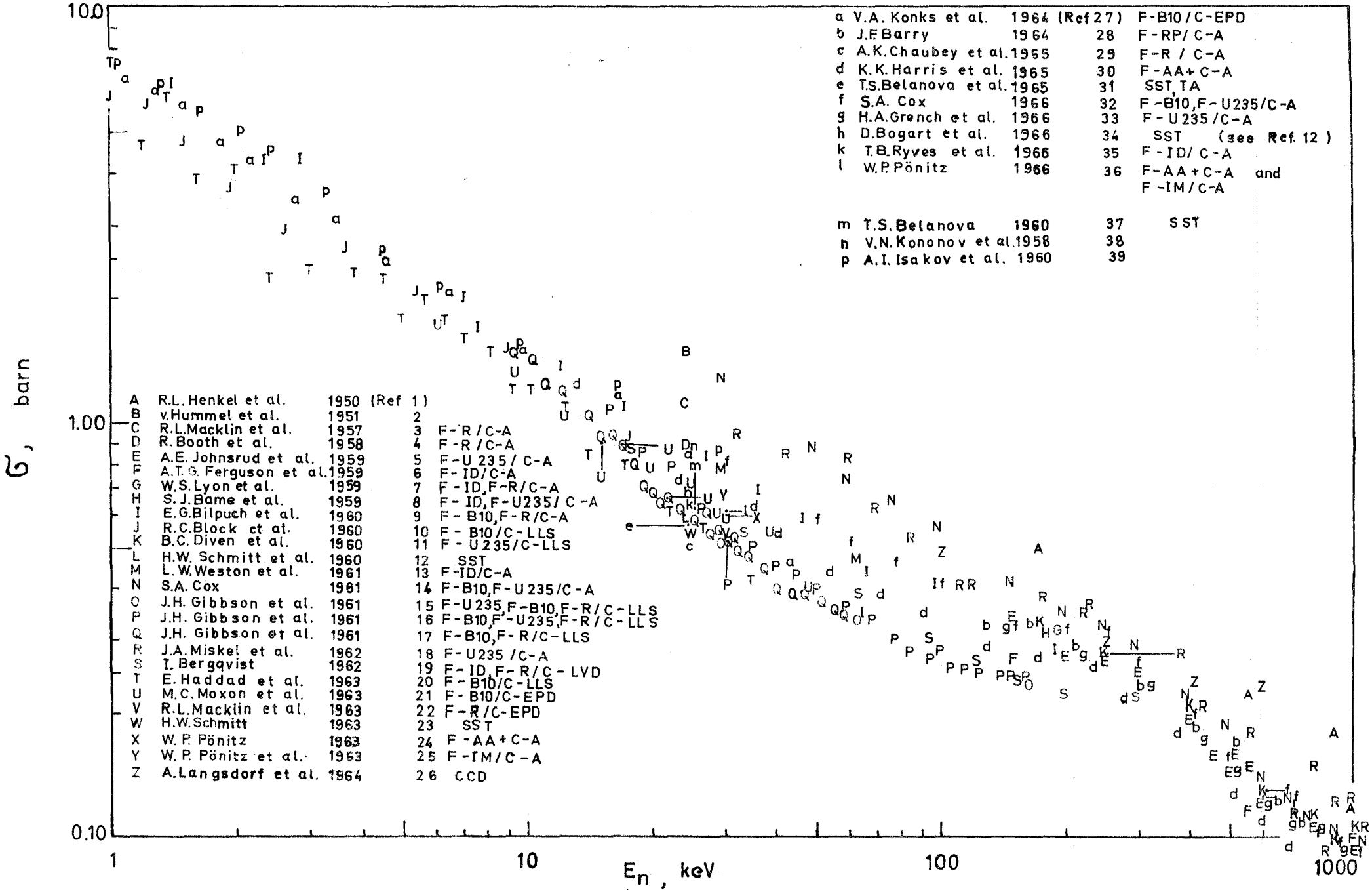

Fig.1 The neutron capture cross section of gold. Comparison of existing data.

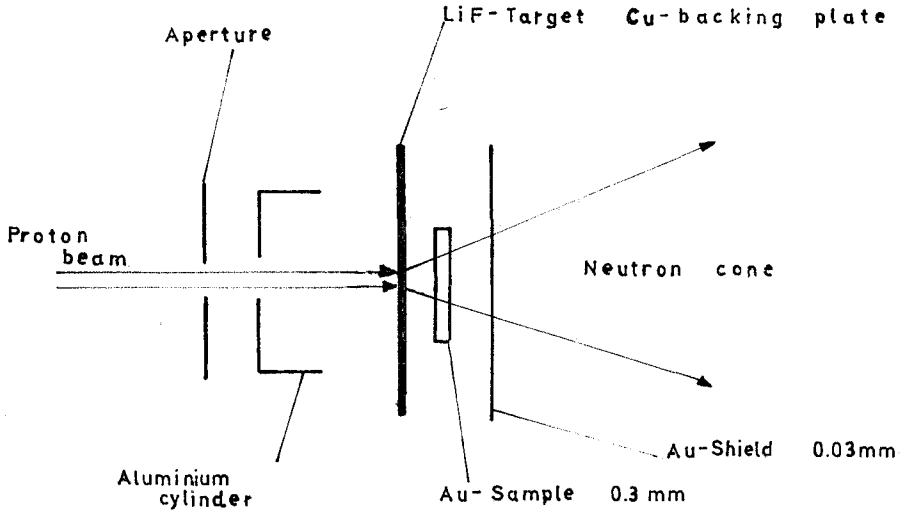

Irradiation arrangement

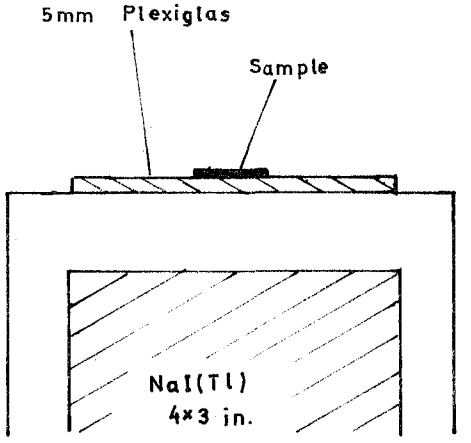

Detector arrangement

1.st Part of the experiment

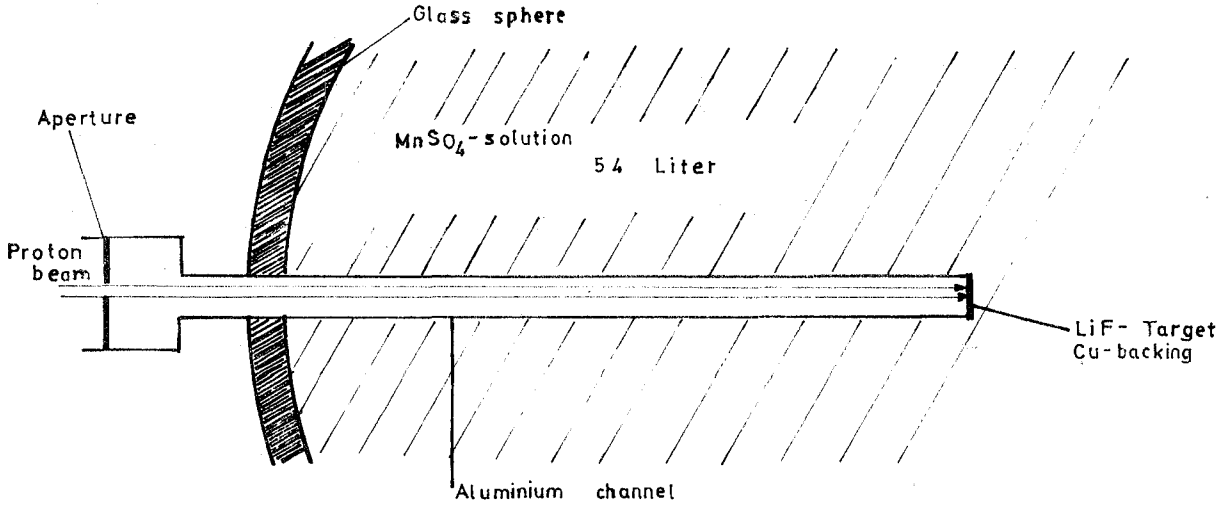

Irradiation arrangement

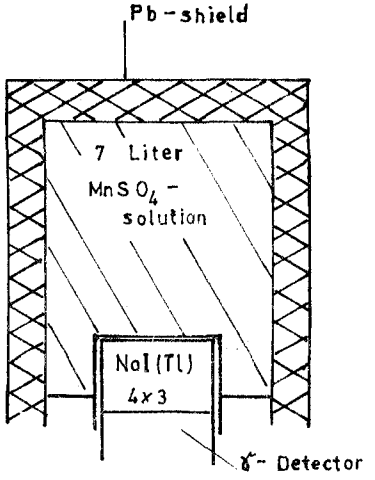

Detector arrangement

2.nd Part of the experiment

Fig. 2 Experimental set-up

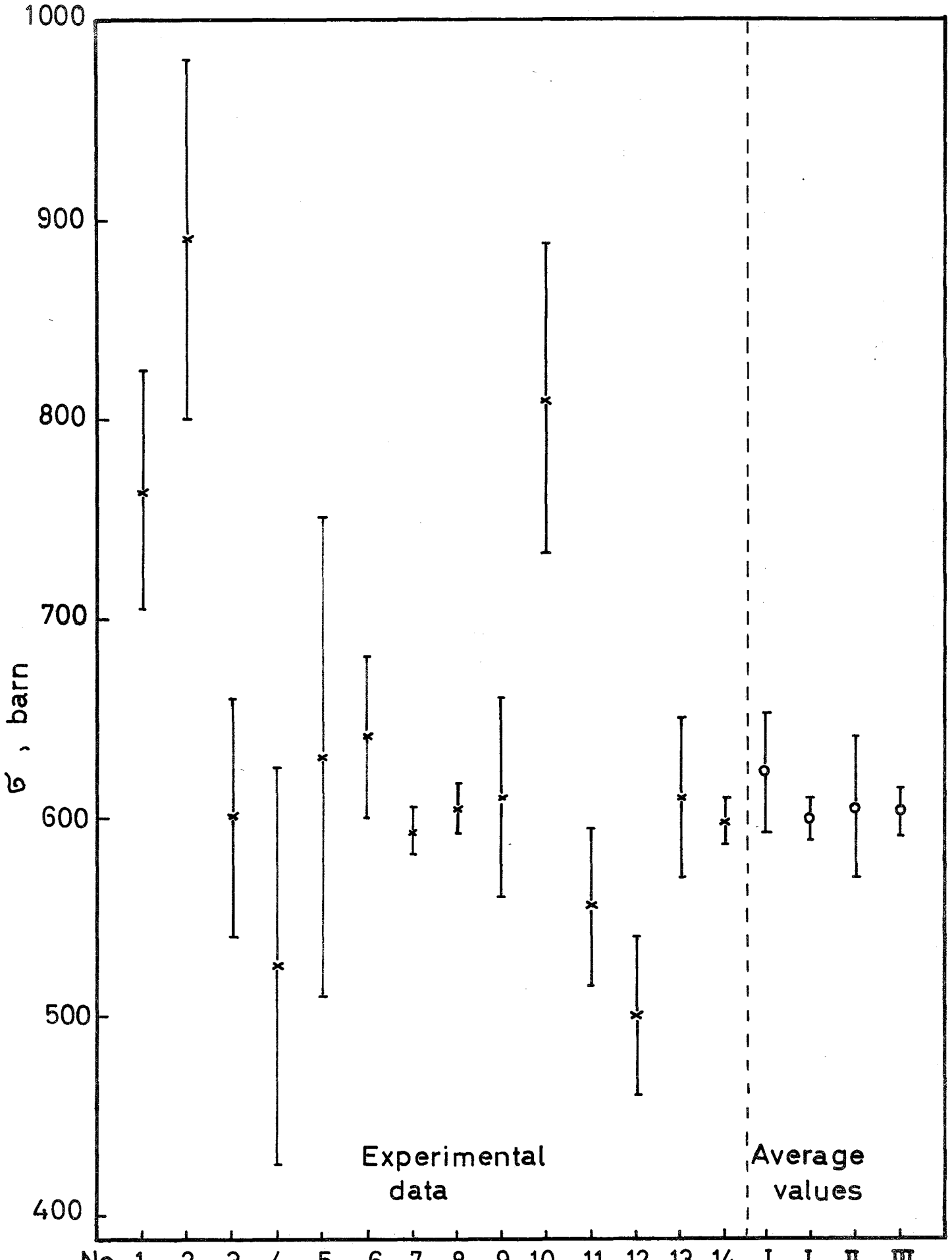

Fig. 3 The independent experimental values of $\sigma_{n,\gamma}^{Au}$ at 30 keV neutron energy.

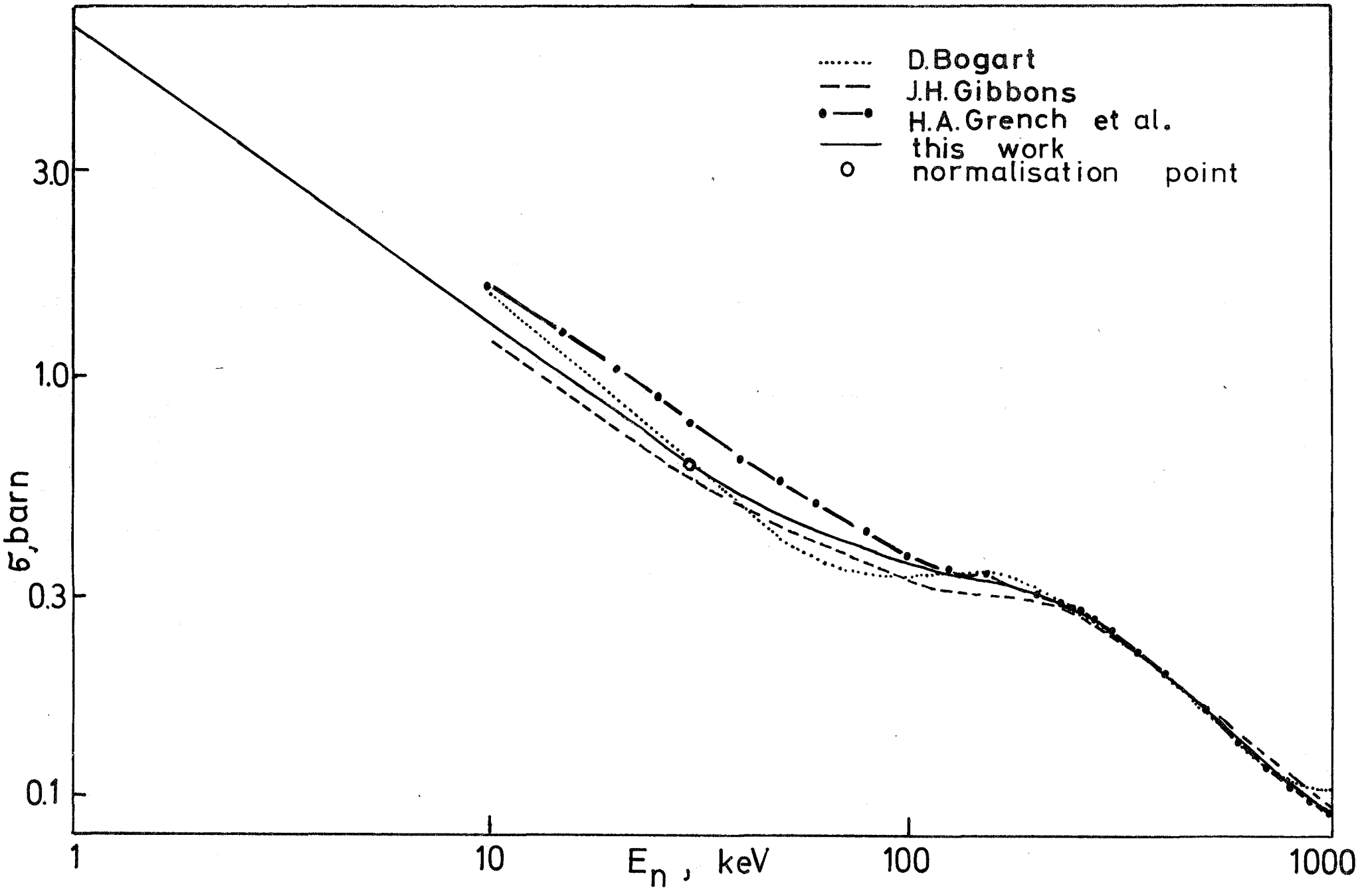

Fig. 4 Comparision of fitted cross section curves.

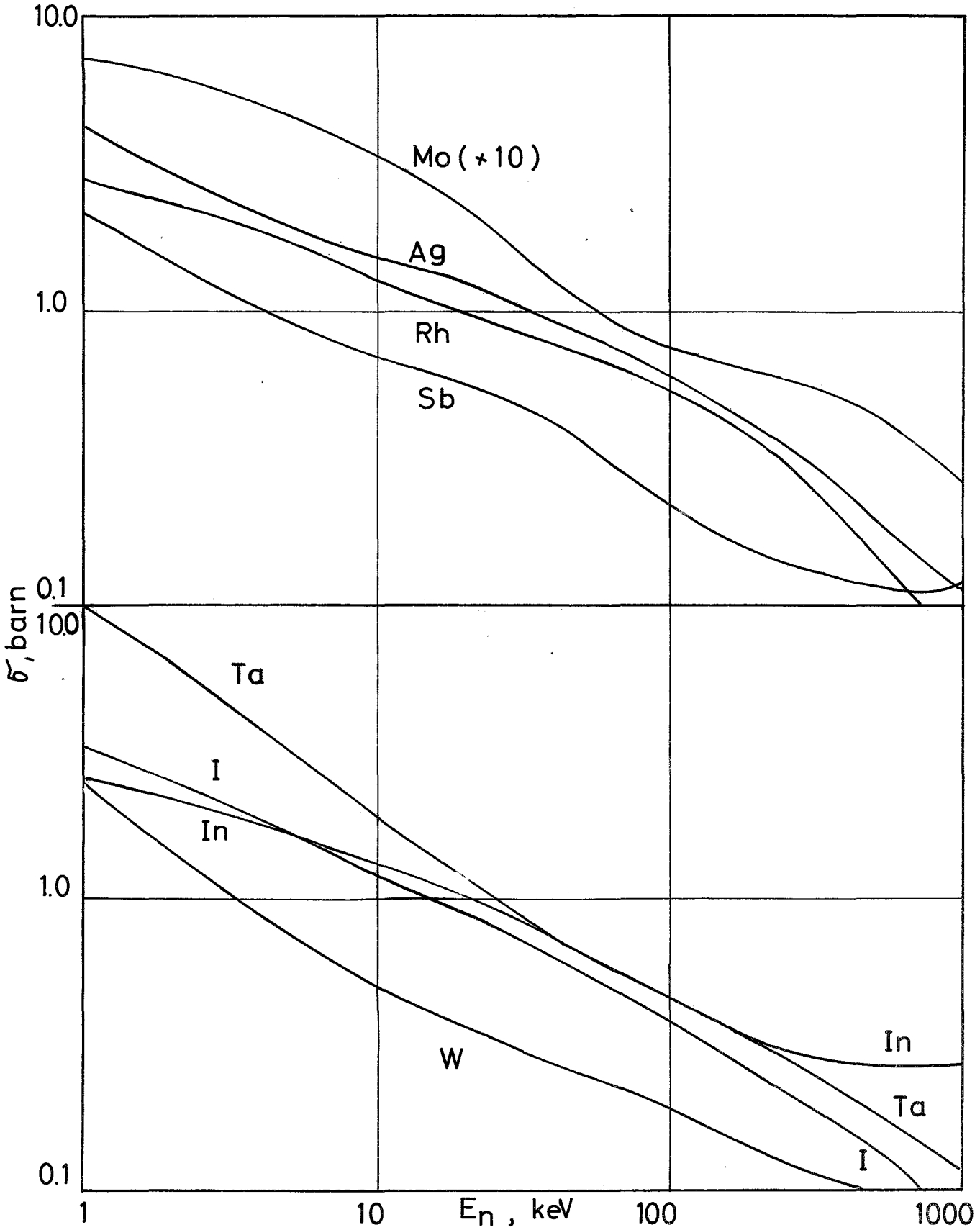

Fig. 5 Capture cross sections of Mo, Rh, Ag, In, Sb, I, Ta and W in the energy range 1-1000 keV